

# $\beta$ -decay studies of neutron rich $^{61-70}\text{Mn}$ isotopes with the new LISOL $\beta$ -decay setup.

J. Van de Walle,<sup>1</sup> N. Bree,<sup>2</sup> J. Cederkäll,<sup>1</sup> P. Delahaye,<sup>1</sup> J. Diriken,<sup>2</sup> V.N. Fedosseev,<sup>1</sup> S. Franchoo,<sup>3</sup> G. Georgiev,<sup>4</sup> O. Ivanov,<sup>2</sup> M. Huyse,<sup>2</sup> U. Köster,<sup>5</sup> Y. Kudryavtsev,<sup>5</sup> B.A. Marsh,<sup>1</sup> D. Pauwels,<sup>2</sup> O. Sorlin,<sup>6</sup> P. Van den Bergh,<sup>2</sup> P. Van Duppen,<sup>2</sup> and W.B. Walters<sup>7</sup>

<sup>1</sup>ISOLDE, CERN, Geneva, Switzerland

<sup>2</sup>Instituut voor Kern- en Stralingsfysica, K.U. Leuven, Leuven, Belgium

<sup>3</sup>IPN Orsay, Orsay Cedex, France

<sup>4</sup>CSNSM, IN2P3-CNRS, Université Paris-Sud, Orsay, France

<sup>5</sup>Institut Laue-Langevin, Grenoble, France

<sup>6</sup>GANIL, Caen, France

<sup>7</sup>Department of Chemistry, University of Maryland, Maryland, USA

The aim of this proposal is to gather new information that will serve as benchmark to test shell model calculations in the region below  $^{68}\text{Ni}$ , where proper residual interactions are still under development. More specifically, the  $\beta$ -decay experiment of the  $^{61-70}\text{Mn}$  isotopes will highlight the development of collectivity in the Fe isotopes and its daughters. At ISOLDE, neutron rich Mn isotopes are produced with a  $\text{UC}_x$  target and selective laser ionization. These beams are particular pure and reasonable yields are obtained for the neutron rich short lived  $^{61-70}\text{Mn}$  isotopes. We propose to perform  $\beta$ -decay studies on  $^{61-70}\text{Mn}$  utilizing the newly developed "LISOL  $\beta$ -decay setup", consisting of two MINIBALL cluster Ge detectors and a standard tape station. The use of digital electronics in the readout of these detectors enables us to perform a "slow correlation technique" which should indicate the possible existence of isomers in the daughter nuclei.

Spokesperson : J. Van de Walle

Contactperson : J. Van de Walle

## I. INTRODUCTION : COLLECTIVITY AROUND $^{68}\text{Ni}$

In recent years, many experiments have investigated the region around the anchor point nucleus  $^{68}\text{Ni}$  (see Fig. 1). The latter nucleus is known for the high excitation energy of the  $2_1^+$  state (2.03 MeV) and the first excited  $0_1^+$  state at 1.7 MeV, together with a low  $B(E2, 2_1^+ \rightarrow 0_1^+)$  value. These three observations have been explained by the semi-magicity of the  $N=40$  neutron sub-shell and the superfluid character of the neutrons near the  $\nu g_{9/2}$  orbit.

In Fig. 2, the experimental  $B(E2, 2_1^+ \rightarrow 0_1^+)$  [W.u.],  $E(2_1^+)$  [MeV] and  $R_{4/2} = E(4_1^+)/E(2_1^+)$  values are summarized for Chromium ( $Z=24$ ), Iron ( $Z=26$ ), Nickel ( $Z=28$ ), Zinc ( $Z=30$ ) and Germanium ( $Z=32$ ) isotopes. The anchor point nucleus  $^{68}\text{Ni}$  is situated at  $Z=28$  and  $N=40$ . Its high  $E(2_1^+)$  is in sharp contrast with the  $E(2_1^+)$  systematics of the neighboring even-even isotopes. Above  $Z=28$ , the  $E(2_1^+)$  of Zinc ( $Z=30$ ) and Germanium ( $Z=32$ ) isotopes decreases for  $38 \leq N \leq 44$  and the  $B(E2)$  values increase to 20 W.u. Both can be interpreted as an increase in collectivity for the Zinc and Germanium isotopes near  $N=40$ . Below  $Z=28$ , the  $2_1^+$  state in Iron ( $Z=26$ ) and Chromium ( $Z=24$ ) isotopes decrease as well, when  $N$  approaches 40. The drop is more pronounced for the Cr isotopes and sets in already near  $N=32$ . In [1], large deformation parameters  $\beta_2$  of 0.3 were derived from the low  $E(2_1^+)$  states in  $^{60,62}\text{Cr}_{36,38}$ . Shell model calculations from the same work indicate large quadrupole moments for both the  $2_1^+$  and  $4_1^+$  states, which are consistent with a deformation parameter of 0.3. Both results are characteristic for axial rotors. Currently few  $B(E2)$  values are known for these nuclei, since these are experimentally hard to measure. Still, apparent collectivity in these medium-heavy nuclei is clear from this systematics.

The apparent collective behavior for  $Z < 28$  was questioned since the  $R_{4/2}$  ratio ( $E(4_1^+)/E(2_1^+)$ ) (Fig. 2C) for the Chromium isotopes is not close to the typical rotational limit of 3.3 [2]. For Fe isotopes, the  $R_{4/2}$  ratio *decreases* from  $N=34$  up to  $N=38$ , contrary to what might be expected if the neutron-rich Fe isotopes were members of a region of increasing deformation as  $N$  approaches 40 [3]. For Zinc ( $Z=30$ ) isotopes, the  $R_{4/2}$  ratio exhibits a typical vibrational behavior. Though,  $B(E2, 4_1^+ \rightarrow 2_1^+)/B(E2, 2_1^+ \rightarrow 0_1^+)$  ratio's in these Zn isotopes are far from the typical value of two for vibrational nuclei [4]. A more microscopic explanation for the apparent collectivity around the  $N=40$  shell gap must be searched for in shell model calculations. In a shell model framework, the increased collectivity is explained by the attractive  $\nu 1g_{9/2} - \pi 1f_{5/2}$  tensor



Z = 31		<sup>61</sup> Ga	<sup>62</sup> Ga	<sup>63</sup> Ga	<sup>64</sup> Ga	<sup>65</sup> Ga	<sup>66</sup> Ga	<sup>67</sup> Ga	<sup>68</sup> Ga	<sup>69</sup> Ga		
		168 ms	116 ms	31.4 s	2.62 m	15 m	9.4 h	78.3 h	67.63 m	stable	β-decay * studied at LISOL □ studied at ISOLDE	
N =		30	31	32	33	34	35	36	37	38		
Z = 28		<sup>60</sup> Ni	<sup>61</sup> Ni	<sup>62</sup> Ni	<sup>63</sup> Ni	<sup>64</sup> Ni	<sup>65</sup> Ni	<sup>66</sup> Ni	<sup>67</sup> Ni	<sup>68</sup> Ni	<sup>69</sup> Ni	<sup>70</sup> Ni
		stable	stable	stable	100(2) y	stable	2.52 h	54.6(3) h	21(1) s	29(2) s	11.4(3) s	6.0(3) s
27		<sup>60</sup> Co	<sup>61</sup> Co	<sup>62</sup> Co	<sup>63</sup> Co	<sup>64</sup> Co	<sup>65</sup> Co*	<sup>66</sup> Co*	<sup>67</sup> Co*	<sup>68</sup> Co*	<sup>69</sup> Co	<sup>70</sup> Co
		1925 d	1.650(5)h	1.50(4)m	27.4(5) s	0.30(3)s	1.20(6)s	0.18(1) s	329(28)ms	0.23(3) s	0.27(5)s	119(6)ms
26		<sup>60</sup> Fe	<sup>61</sup> Fe	<sup>62</sup> Fe	<sup>63</sup> Fe	<sup>64</sup> Fe	<sup>65</sup> Fe*	<sup>66</sup> Fe*	<sup>67</sup> Fe*	<sup>68</sup> Fe	<sup>69</sup> Fe	<sup>70</sup> Fe
		1.5E6 a	5.98(6)m	68(2)s	6.1(6) s	2.0(2) s	1.07(12)s	830(80)ms	411(32)ms	132(39)ms	0.17(3)s	94(17) ms
25		<sup>60</sup> Mn	<sup>61</sup> Mn	<sup>62</sup> Mn	<sup>63</sup> Mn	<sup>64</sup> Mn	<sup>65</sup> Mn	<sup>66</sup> Mn	<sup>67</sup> Mn	<sup>68</sup> Mn	<sup>69</sup> Mn	<sup>70</sup> Mn
		0.28(2)s	623(10)ms	671(5) ms	0.29(2) s	90(4) ms	88(4) ms	66(4) ms	47(2) ms	28(4) ms	14(4) ms	
N =		35	36	37	38	39	40	41	42	43	44	45

FIG. 1: Selected part of the chart of nuclei, focusing on the region around the anchor point nucleus <sup>68</sup>Ni and the isotopes with Z<28. Ga isotopes which will form an isobaric background at ISOLDE are shown as well, indicating the large difference in half lives.

interaction and the repulsive  $\nu 1g_{9/2}-\pi 1f_{7/2}$  interaction. This interaction reduces the N=40 and Z=28 shell gaps, thereby enhancing p-h excitations. The large B(E2) value for <sup>70</sup>Ni (Z=28,N=42) is an illustrative example of this reduction, since shell model calculations allowing f<sub>7/2</sub> protons to scatter across the Z=28 gap underestimate the quadrupole collectivity value.

The main difficulty in the shell model approach is the large valence space for the nucleons, which brings in a computational problem. Recent theoretical efforts by Caurier *et al.* [5] have illustrated the influence of a larger valence space on the calculated E(2<sub>1</sub><sup>+</sup>). For both Fe and Cr isotopes, the lowering of the 2<sub>1</sub><sup>+</sup> state is *only* reproduced when considering the pfgd valence space (considering <sup>52</sup>Ca as closed core and including g<sub>9/2</sub> and 2d<sub>5/2</sub> neutron orbitals).

ETFSI calculations from [6] yield a deformation parameter  $\beta_2$  between 0.2 and 0.3 for the neutron-rich Fe and Mn isotopes. From the level scheme of <sup>66</sup>Co, resulting from the recent  $\beta$ -decay experiment of <sup>66</sup>Fe at the LISOL facility, a value of  $\beta_2 \sim 0.3$  was inferred for the ground state deformation of <sup>66</sup>Fe [7], which seems to confirm the assumption of large deformation in the neutron rich Fe isotopes.

It is clear that the collective behavior around N=40 is related to the gradual occupancy of the  $\nu 1g_{9/2}$  orbital. This orbit is therefore believed to be the "shape driving" orbital in this mass region. The presence of this positive parity orbital near the negative parity f<sub>5/2</sub>p<sub>3/2</sub>p<sub>1/2</sub> shell (pf-shell) and its high j-value, compared to the underlying negative parity pf orbitals, is also responsible for isomerism in this region of the nuclear chart. Indeed, many isomers have been observed in this region with half lives ranging from several 10<sup>-3</sup> s to 10<sup>-9</sup>s [8, 9]. In some cases even ranging up to several seconds (ex. <sup>70</sup>Cu<sub>41</sub>).

*With this proposal, we intend to investigate the structure of neutron rich Fe isotopes and its decay (grand-)daughters (see Fig. 1), by means of gamma spectroscopy following  $\beta^-$ -decay of neutron rich Mn isotopes. A new  $\beta$ -decay setup based on two triple segmented MINIBALL detectors, plastic detectors, a tape system, heavy shielding and digital electronics will be used. With the new setup, isomers which are fed in the direct  $\beta^-$ -decay as well as in the delayed neutron emission channel can be identified with the "slow correlation technique" [10]. In order to obtain a complete picture it is crucial that all relevant masses (A=61-70) are investigated with the same setup and long enough measuring cycles are employed as to monitor longer lived activity as well. In the region around <sup>68</sup>Ni, several Fe, Co, Ni and Cu isotopes have already been studied by means of gamma spectroscopy following  $\beta$ -decay. Since the region below Z<28 is believed to contain isomers, it is crucial to extend these studies to lower Z (Manganese) isotopes as to obtain information in their position and lifetime.*

In the following, an overview will be given of the current knowledge on the isotopes of interest, the current physics interest will be highlighted and achievements of previous studies, utilizing the same setup, are described to indicate the suitability of this setup in this region of the nuclear chart.

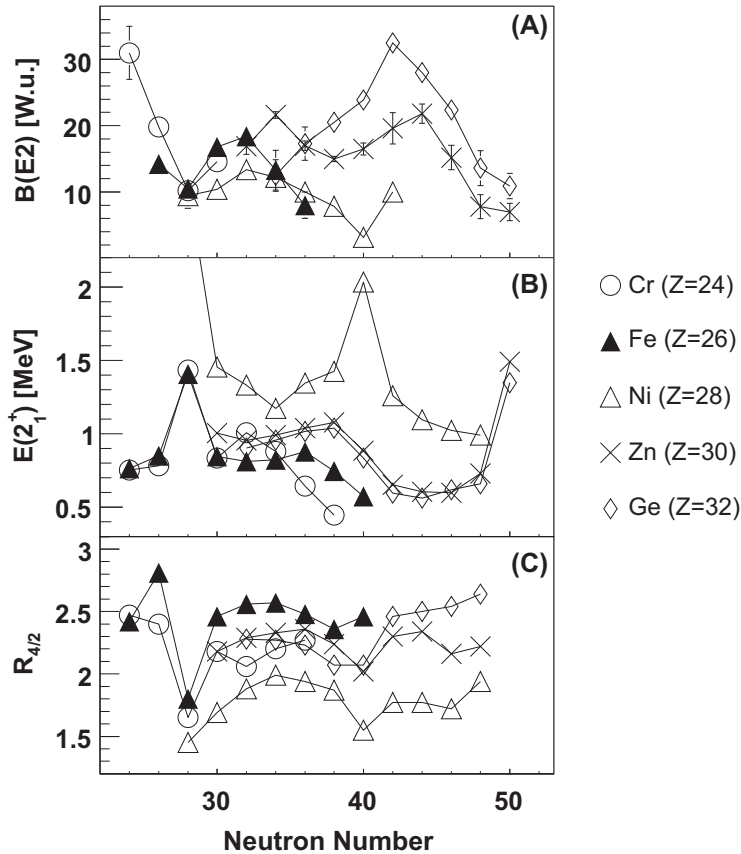


FIG. 2:  $B(E2)$  [W.u.],  $E(2_1^+)$  and  $R_{4/2}$  of Chromium ( $Z=24$ ), Iron ( $Z=26$ ), Nickel ( $Z=28$ ), Zinc ( $Z=30$ ) and Germanium ( $Z=32$ ) isotopes. Data taken from [1, 4, 9, 11, 12].

## II. PHYSICS CASES

### A. Structure of even mass Fe isotopes ( $A=62,64,66,68$ )

#### 1. $A=62$

In [13] an unknown short lived 84(10) ms activity was observed in the  $\beta$  count rate accumulated at the  $A=62$  mass chain, whereas both  $\beta$  as neutron counters showed a 670(5) ms component. This indicates the presence of a short lived isomer in  $^{62}\text{Mn}$ . No gamma-ray data was taken at that time. In repeating this  $A=62$  experiment with the dedicated  $\beta$ - $\gamma$  setup, this issue can possibly be clarified from the observed gamma rays and their time behavior.

#### 2. Earlier Studies at ISOLDE ( $A=64,66$ )

In 1998,  $^{60-69}\text{Mn}$  isotopes were produced and brought to the Mainz neutron detector and a  $\beta$ -counter [13, 14]. This experiment yielded half lives and  $P_n$  values for 10 Mn isotopes ( $A=60-69$ ) and two isomeric states in  $^{60,62}\text{Mn}$ . Parallel to this experiment, aiming at the measurement of  $P_n$  values, the beam was sent to a tape station where single gamma rays (no beta-gating was applied) following the  $\beta$ -decay of  $^{64,66}\text{Mn}$  were monitored. The gamma detection resulted in a level scheme of  $^{64,66}\text{Fe}$  (see Fig. 3), where the  $2_1^+$  states in both isotopes were established and confirmed by in-beam studies [15]. The discovery of these states was the first indication that collectivity sets in earlier in neutron rich Fe isotopes, compared to  $Z>28$  isotopes

(see paragraph I). The identification of gamma lines belonging to the decay of Mn was based on "early" and "late" coincidences (gamma spectra were written in 100 ms time slices). Several gamma lines in the "late" spectrum remain unidentified and are possibly originating from  $\beta$ -decay of the daughter products.

With new technology developed over the last 10 years, based on segmented particle and  $\gamma$  detectors and digital electronics [10], it has become possible to *continuously monitor the gamma decay in absolute time* and the "slow correlation technique" permits to *monitor the time behavior of each line individually and with respect to other decay lines* and this within the seconds range, provided clean sources are delivered to the detection system. The "slow correlation technique" was utilized for the first time in a  $\beta$ -decay study of  $^{67}\text{Fe}$  at the LISOL setup in the CRC (Louvain-la-Neuve, Belgium) [10]. An isomeric state at 492 keV was populated in the daughter nucleus  $^{67}\text{Co}$ , and a half life of 494(24) ms was determined for this isomer, which is similar to the half life of the  $^{67}\text{Co}$  ground state (329(28) ms). This example nicely illustrates the power of the new setup. An improvement compared to the 1998 experiment is the usage of selective  $\beta$ -gating (*without losing the singles data*), which can clean the spectrum additionally.

We propose to use 2 shifts on the remeasurement of  $^{64,66}\text{Mn}$  beta decay, this to test the new setup, to establish the results from 1998 and to have a reference measurement taking into account the  $P_n$  branches in the decay of neighboring  $^{65,67}\text{Mn}$ , which are considerable (see Table I).

### 3. $A=68,70$

No gamma-rays are known in the  $\beta$ -decay of  $^{68,70}\text{Mn}$ . In both cases, life times  $<28$  ms are expected, so gamma rays can be searched for in the first few ms after the proton pulse. It should be possible to determine the energy of the first excited  $2_1^+$  state in  $^{68}\text{Fe}$  (see Fig. 2B), which should be the most intense gamma line in this decay, with the currently available intensity of  $^{68}\text{Mn}$ . Firm identification of this gamma ray will be based on laser on/off measurements. The  $\beta$ -decay of the daughter product  $^{68}\text{Fe}$  is in itself interesting since 10 gamma rays are known in its decay to the long lived isomer in  $^{68}\text{Co}$  [16], but no level scheme could be constructed due to lacking coincidences and statistics. Again, the  $P_n$  branch of the  $^{68}\text{Mn}$  decay (not measured, but theoretically predicted to be 14-20 %) can populate different spin states in  $^{67}\text{Fe}$ , compared to the direct  $\beta$ -decay of  $^{67}\text{Mn}$ . Since the ground state spin of  $^{67}\text{Fe}$  is either  $(5/2^+)$  [17] or  $(3/2^-)$  [10], this could provide valuable additional information on the different spin states in this nucleus. No yield is known for  $^{70}\text{Mn}$  and it is expected to be  $<1$  atom/ $\mu\text{C}$ . By using a very short measuring cycle ( $^{70}\text{Ga}$  contaminant has  $T_{1/2}=21.2$  m) and restricting the  $\beta$ - $\gamma$  coincidences to the first few ms after the proton impact, an indication for the  $2_1^+$  state should be within reach in two shifts.

## B. Structure of odd mass Fe isotopes ( $A=61,63,65,67,69$ )

### 1. $A=61,63$

The level structure of both  $^{61,63}\text{Fe}$  is poorly known. In addition, the direct  $\beta$ -decay of  $^{61,63}\text{Mn}$  is important in order to have a reference when searching for gamma-rays associated with the  $P_n$  branch of  $^{62,63,64}\text{Mn}$ .

### 2. $A=65$

In  $^{65}\text{Fe}_{39}$ , evidence has been found for two isomeric states (see Fig. 4). In [8] a state at 364 keV has been reported with a lifetime of  $0.43(13)$   $\mu\text{s}$  and spin  $(5/2^-)$ . Recent results from GANIL [16] show that this 364 keV level is only slightly retarded (some ns) and an alternative isomeric level at 397 keV is postulated with a similar half life of  $420(13)$  ns and a spin of  $1/2^+$ . The level at 364 keV is directly fed by the  $\beta$ -decay from the  $(5/2^-)$  ground state of  $^{65}\text{Mn}$  and is proposed to have a spin  $(1/2^-, 3/2^-)$ . No gamma-gamma coincidences were observed in the  $\beta$ -decay experiment performed at GANIL. A band structure is observed in [15], which is believed to be build on a  $9/2^+$  state at unknown excitation energy. This state could be a second isomeric state. In a recent  $\beta$ -decay experiment at LISOL, two structures are observed in the decay of the produced  $^{65}\text{Fe}$ . These two independent structures might originate from the decay of the ground state :  $(3/2^-)$  [18],  $(5/2^-)$  [16], and a long lived isomeric state in  $^{65}\text{Fe}$  which could be the  $(9/2^+)$  state hinted in

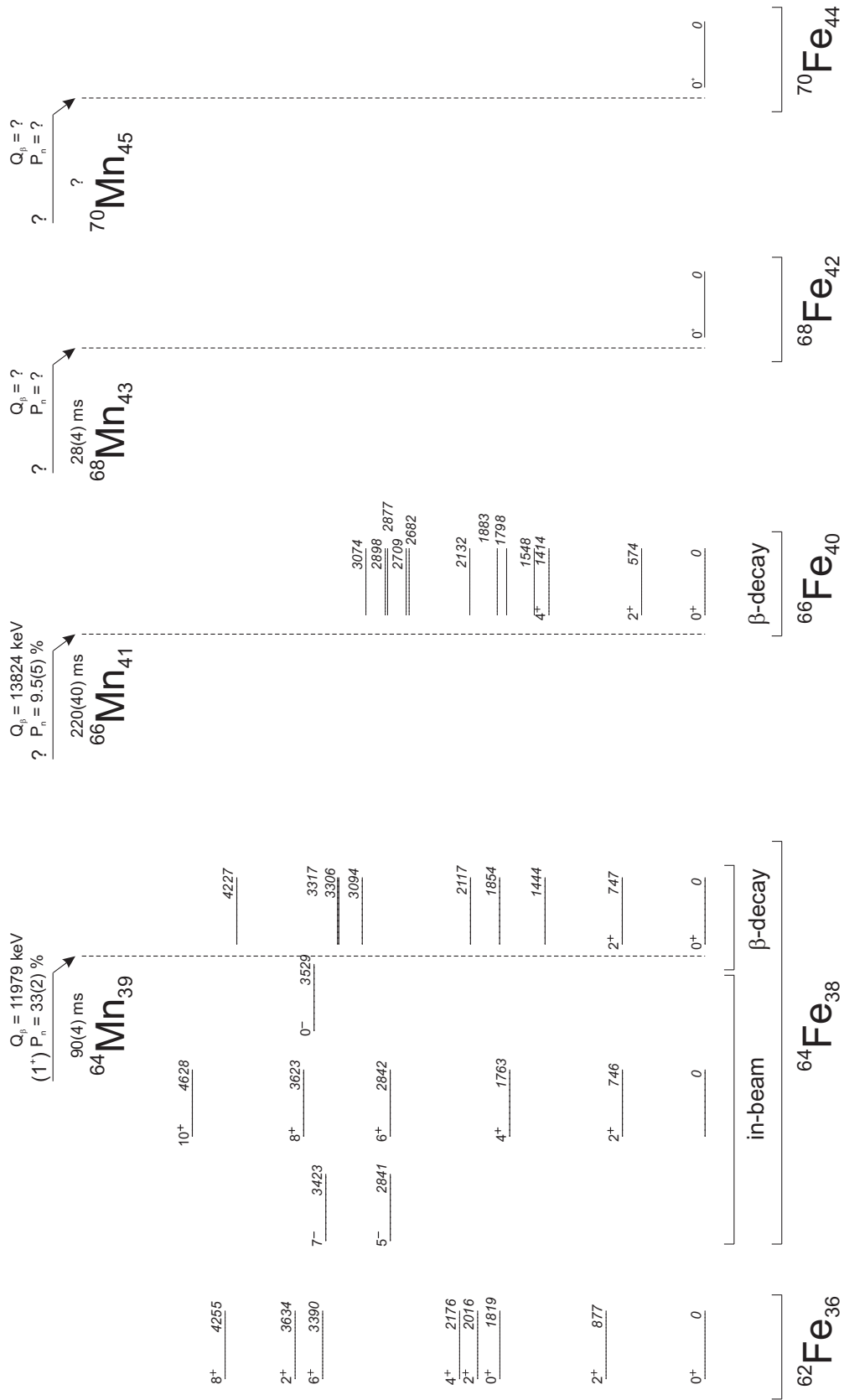


FIG. 3: Nuclear structure of  $^{64,66,68}\text{Fe}$  isotopes. Data is taken from [3, 7, 9, 13, 15]. The level structure is plotted according to the experimental probe (in-beam and  $\beta$ -decay). For clarity, log ft and  $\beta$  branching ratio's are omitted for the  $\beta$ -decay data.

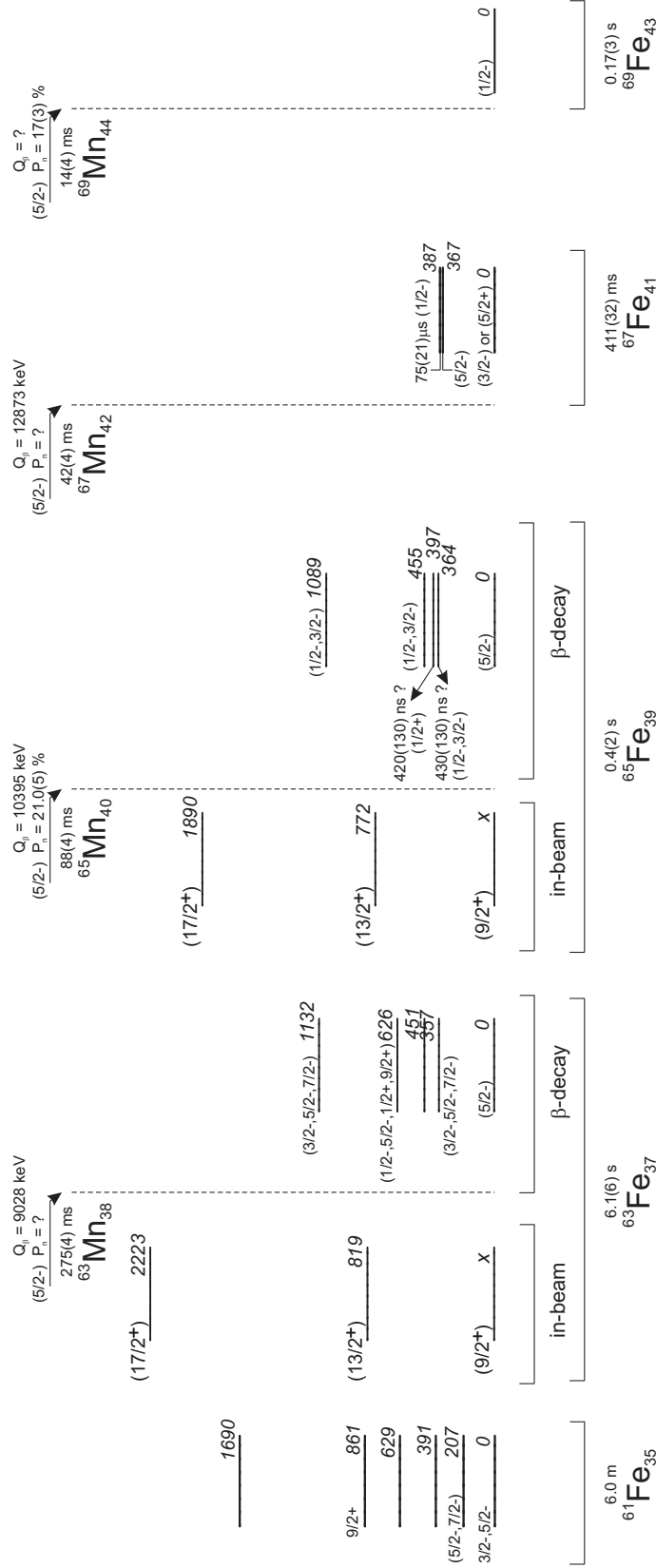


FIG. 4: Nuclear structure of  $^{63,65,67,69}\text{Fe}$  isotopes. Data is taken from [9, 13, 15, 16, 18]. The level structure is plotted according to the experimental probe (in-beam and  $\beta$ -decay). For clarity, log ft and  $\beta$  branching ratio's are omitted for the  $\beta$ -decay data.

[15]. Evidence for an isomeric state in  $^{65}\text{Fe}$  at 402(5) keV and a half life of  $> 150$  ms has also been found in mass measurements at MSU and could again be the  $(9/2^+)$  state.

The  $\beta$ -decay of  $^{65}\text{Mn}$  (half life of 88(4) ms and ground state spin of  $(5/2^-)$  [16]) will yield more insight in the level structure of  $^{65}\text{Fe}$ . Additionally, the beta delayed neutron emission branch in the decay of  $^{66}\text{Mn}$  ( $P_n=9.5(5)\%$ ) will populate different spin states.

### 3. $A=67$

In  $^{67}\text{Fe}$ , two states are known at 367 and 387 keV [17] (see Fig. 4). In [8] the state at 367 keV was assigned a spin  $(5/2^-)$  and an isomeric half life of 43(30)  $\mu\text{s}$ . In [17], this was questioned and the state at 387 keV was assigned spin  $(1/2^-)$  with a half life of 75(21)  $\mu\text{s}$ , whereas the spin of the 367 keV level remained  $(5/2^-)$ . The ground state spin of  $^{67}\text{Fe}$  was assigned  $(5/2^+)$  in [17]. This spin sequence is now questioned again, since from recent  $\beta$ -decay studies at LISOL of  $^{67}\text{Fe}$ , a ground state spin of  $(3/2^-)$  was deduced [18]. In [16], four gamma rays (367,387,940,1568 keV) are reported in the decay of  $^{67}\text{Mn}$ . Contrary to [8, 17], the 367 keV and 387 keV gamma rays are found not to be retarded and a higher lying isomeric level is postulated, close to 387 keV ( $<30$  keV higher). The pure source of  $^{67}\text{Mn}$  (the contaminant  $^{67}\text{Ga}$  is much longer lived (78 h, see Fig. 1), available at ISOLDE and the new  $\beta$ -decay setup, allowing improved  $\gamma$ - $\gamma$  coincidence conditions (see Section III), can shed light on this standing problem.

### 4. $A=69$

In the mass chain 69, no spectroscopic information is available for Fe and Co. With a half life of 14(4) ms and a production yield of 1 per  $\mu\text{C}$  proton beam, this mass chain is at the limit of feasibility. The main isobaric contaminant,  $^{69}\text{Ga}$ , is stable, so no contaminating gamma rays are expected in this case. A very clean spectrum is expected for this short lived isotope and all its daughter decay products. Two gamma rays were already observed at GANIL in the  $\beta$ -decay of  $^{69}\text{Fe}$  (249 keV and 1879 keV), but no level scheme was constructed.

## III. THE EXPERIMENTAL SETUP

A new experimental setup, illustrated in Fig. 5, will be used for the first time at ISOLDE. This setup has been developed at KU Leuven and used at LISOL, at the CRC facility in Louvain-la-Neuve, to investigate the  $\beta$ -decay properties of  $^{65,66,67}\text{Fe}$ . In this new setup, the gamma detectors are replaced by two "MINIBALL"-type Germanium detectors, each consisting of three segmented crystals. The two detectors are read out with digital electronics. The main advantage of the latter is the capability to continuously monitor incoming gamma ray and  $\beta$ -trigger data. Each event (gamma as well as beta) acquires a time stamp during the data taking (this can be referred to as "trigger-less" data taking). Any conditioning to additionally clean the gamma spectra is performed off-line. The "slow correlation technique", which is described in [10], allows to identify isomers in the seconds range which are fed by  $\beta$ -decay but are lost when requiring a prompt coincident with a  $\beta$ -particle on-line. The total  $\gamma$ -detection efficiency is  $\sim 5\%$  at 1 MeV and the total  $\beta$ -detection efficiency is  $\sim 45\%$ .

The segmentation of the germanium crystals is crucial in the suppression of true-coincidence summing events, which are problematic when non-segmented coaxial Germanium detectors are used at close distance from the source. At the same time, the segmentation allows further to increase the probability for gamma-gamma (or even  $\beta$ -gamma-gamma) coincidences.

Therefore, this setup is ideally suited to study the  $\beta$ -decay from Manganese ( $Z=25$ ) down to Iron ( $Z=26$ ), Cobalt ( $Z=27$ ) and Nickel ( $Z=28$ ). This new setup is an important improvement compared to the setup utilized in the 1998 experiment. The improved detection efficiency, the segmentation of the Ge crystals and the "trigger-less" data taking are further important improvements, compared to other experimental setups.

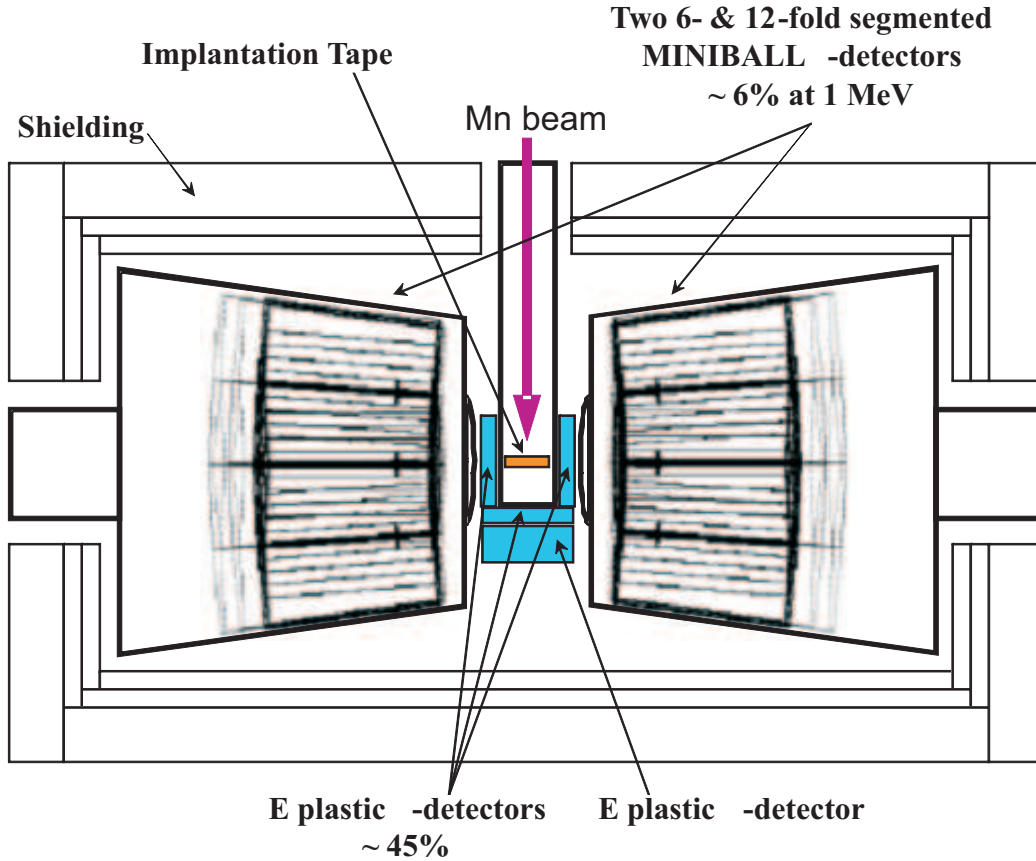


FIG. 5: Schematic overview of the LISOL  $\beta$ -decay setup, utilizing two MINIBALL Germanium detectors, each consisting of three segmented Ge crystals. (Picture taken from [7])

A	Yield/ $\mu\text{C}$	$T_{1/2}$ [ms]	$P_n$ [%] [13]	$\beta$ - $\gamma$ Cts/shift	$\beta$ - $\gamma$ Cts/shift in $P_n$ branch
61	1.7E6	670(40) [9]	0.6(1)	3.7E9	2.3E7
62	7.0E5	671(5) [13]	2.9(5)	1.5E9	4.5E7
63	2.0E5	275(4) [13]	30.5(5)	3.1E8	1.4E8
64	7.0E3	90(4) [9]	33(2)	1.0E7	5.1E6
65	1.0E3	88(4) [13]	21.0(5)	1.8E6	4.7E5
66	1.7E2	66(4) [13]	9.5(5)	3.4E5	3.6E4
67	1.0E2	47(2) [9]	26*	1.7E5	5.5E4
68	4.0E0	28(4) [13]	19*	7.2E3	1.7E3
69	1.0E0	14(4) [13]	17(3)	1.8E3	3.8E2

TABLE I: Expected count rates for the investigated masses. Assuming a  $2 \mu\text{A}$  proton beam and no losses in the transmission from target to tape station. Yields are taken from the ISOLDE yield data base, half lives and  $P_n$  values from [9, 13] (\**theoretical value*). Count rates are given for a gamma ray at 500 keV taking into account 45%  $\beta$ -detection efficiency [7] and 8.6%  $\gamma$ -ray detection efficiency. This for both direct  $\beta$ -decay ( $1-P_n$ ) and the  $\beta$ -delayed neutron emission branch.

#### IV. YIELDS AND BEAM TIME REQUEST

The Mn beams at ISOLDE are produced with a **UC<sub>x</sub> target and selective laser ionization**. The laser ionization efficiency for manganese is  $\sim 19\%$  and is one of the highest for any element produced with RILIS. The yields for neutron rich Mn isotopes are summarized in table I. The main anticipated contaminant is Ga for all considered masses. In the 1998 experiment, with a 1 GeV proton beam, yields of Mn isotopes exceeded those of the Ga isotopes up to mass 63. With a 1.4 GeV proton beam, the yield of neutron-



deficient Ga isotopes might be slightly higher. Though, **by applying macro-gating of the released atoms**, i.e. applying a beam gate for three half lives of the considered Mn isotopes, the gamma background from radioactive Ga isotopes can be suppressed. Additionally, micro-gating (i.e. gating the laser ionized atoms between two laser pulses) can increase considerably the Mn/Ga ratio. Contaminating radioactivity from isobaric Ga contaminants is limited as well due to their long half lives, compared to Mn and its decay daughters (see Fig. 1). For A=63-69, the Mn activity is roughly comparable to the Ga activity within one half life of the Mn isotopes. Laser off data, which will be taken on each mass, provides a strong selectivity in the observed gamma rays.

The **use of the HRS is mandatory**, especially for the  $^{69}\text{Mn}$  beam, in order to exclude tiny tails of neighboring masses. Though, this beam should be clean ( $^{69}\text{Ga}$  is stable) as it comes to gamma detection. The use of a long implantation tape permits to carry away the long lived activity from Ga isotopes after each measuring window. We aim to measure the  $\beta$ -decay of  $^{64,66,68}$ ,  $^{65,67,69}\text{Mn}$  and short lived daughter products.

The neutron background in the experimental hall after the proton impact induces background in the data. Therefore, the optimal position of the experimental setup would be the furthest possible from the HRS. The installation of the experimental setup should take up to 1 week.

In order to be able to apply the "slow correlation technique" on the data, it is necessary to acquire sufficient statistics on all masses. At the same time, sufficient laser off data needs to be taken, in order to achieve a good selectivity in the observed gamma rays. Therefore, we would need **1 shift for each  $^{61,62,63,64,65,66,67}\text{Mn}$  isotope and 16 shifts in total for  $^{68,69,70}\text{Mn}$  decay**. These estimates are based on experience at the CRC with this setup, where the  $^{67}\text{Fe}$   $\beta$ -decay experiment utilized 50 hours ( 6 shifts) of data taking with 1.25 atoms/sec implanted on the tape. **One shift should be dedicated to the optimization of the beam parameters.**

In total we ask for **24 shifts** to perform this  $\beta$ -decay experiment on neutron rich Mn isotopes.

- 
- [1] O. Sorlin *et al.*, Eur. Phys. J. A **16**, 55 (2003).
  - [2] S. Zhu *et al.*, Phys. Rev. C **74**, 064315 (2006).
  - [3] N. Hoteling *et al.*, Phys. Rev. C **74**, 064313 (2006).
  - [4] J. Van de Walle *et al.* (2007), in preparation.
  - [5] E. Caurier *et al.*, Eur. Phys. J. A **15**, 145 (2002).
  - [6] Y. Aboussir *et al.*, At. Data and Nucl. Data Tables **61**, 127 (1995).
  - [7] O. Ivanov, Ph.D. thesis, K.U. Leuven (2007).
  - [8] R. Grzywacz *et al.*, Phys. Rev. Lett. **81**, 766 (1998).
  - [9] URL <http://www.nndc.bnl.gov/nndc/nudat/>.
  - [10] D. Pauwels *et al.* (2007), subm. to Nucl. Instr. Meth. B.
  - [11] E. Padilla-Rodal *et al.*, Phys. Rev. Lett. **94**, 122501 (2005).
  - [12] A. Gadea *et al.*, Presentation at the Zakopane Conference on Trends in Nuclear Physics, Poland (2006).
  - [13] M. Hannawald, Ph.D. thesis, Universitat Mainz (2000).
  - [14] M. Hannawald *et al.*, Phys. Rev. Lett. **82**, 1391 (1999).
  - [15] S. Lunardi *et al.*, Phys. Rev. C **76**, 034303 (2007).
  - [16] L. Gaudefroy, Ph.D. thesis, Universite Paris XI Orsay (2005).
  - [17] M. Sawicka *et al.*, Eur. Phys. J. A **16**, 51 (2003).
  - [18] D. Pauwels, M. Huysse, P. Van Duppen, and O. Ivanov (2007), private communication.